Comparison of sector field- and quadrupole-ICP-MS for the determination of DBT and TBT in sediment following GC separation

Yang, L.; Mester, Z.; Sturgeon, R.

Publisher's version / Version de l'éditeur:
https://doi.org/10.1039/b304705a
Journal of Analytical Atomic Spectrometry, 18, 11, pp. 1365-1370, 2003

JAAS FULL PAPER
www.rsc.org/jaas

Comparison of sector field- and quadrupole-ICP-MS for the determination of DBT and TBT in sediment following GC separation†

Lu Yang,* Zoltán Mester and Ralph E. Sturgeon

Institute for National Measurement Standards, National Research Council Canada, Ottawa, Ontario, Canada K1A 0R6. E-mail: Lu.Yang@nrc.ca

Received 28th April 2003, Accepted 27th August 2003
First published as an Advance Article on the web 8th September 2003

A method is described for the accurate and precise determination of tributyltin (TBT) and dibutyltin (DBT) by species-specific isotope-dilution plasma-source mass spectrometry. Using gas chromatography (GC) for sample introduction and analyte separation, a performance comparison was made between sector field inductively coupled plasma mass spectrometry (SF-ICP-MS) detection and quadrupole ICP-MS (qICP-MS) detection. Samples were extracted with acetic acid using open microwave digestion, derivatized with sodium tetraethylborate and extracted into isooctane. Mass bias correction was implemented based on the expected ratio of $^{120}Sn/^{117}Sn$ to that of the mean $^{120}Sn/^{117}Sn$ ratio calculated from the inorganic Sn peaks detected in all chromatograms. A more than 2-fold improvement in precision of calculated $^{120}Sn/^{117}Sn$ ratios was obtained for both TBT and DBT in standards using GC-SF-ICP-MS as compared to GC-qICP-MS. PACS-2 certified reference material marine sediment (NRCC, Ottawa, Canada) was used for method validation. Concentrations of 0.883 $\pm$ 0.013 and 1.126 $\pm$ 0.013 μg g^{-1} (mean and one standard deviation, $n = 4$) as tin were obtained for TBT and DBT, respectively, using GC-SF-ICP-MS detection, in agreement with the certified values of 0.98 $\pm$ 0.13 and 1.09 $\pm$ 0.15 μg g^{-1} (95% confidence interval), respectively. Concentrations of 0.883 $\pm$ 0.019 and 1.116 $\pm$ 0.014 μg g^{-1} (mean and one standard deviation, $n = 4$) as tin were obtained for TBT and DBT, respectively, using GC-qICP-MS detection. Slightly better precisions of 1.59–1.62% RSD for TBT and DBT in a test sediment were obtained using GC-SF-ICP-MS compared with 1.64–3.31% RSD obtained with GC-qICP-MS. Method detection limits (LODs, three times standard deviation) of 0.4 and 0.3 ng g^{-1} for TBT and DBT, respectively, were obtained using GC-SF-ICP-MS, based on processing a 0.5 g sample. As expected, these are superior to LODs of 0.9 and 1.0 ng g^{-1} obtained using GC-qICP-MS, arising from the three-fold enhancement in signal-to-background ratio obtained with the sector field machine.

Introduction

Since 1983, following its commercialization, quadrupole based inductively coupled plasma mass spectrometry (qICP-MS) has been widely used for trace and ultra-trace element determinations[1] due to its high sensitivity, large dynamic range and multi-element capability. Moreover, if two interference-free isotopes of a given element are available, the isotope dilution (ID) calibration strategy can be applied, which generally provides superior accuracy and precision over other calibration strategies, including external calibration and standard additions. This arises because a ratio, rather than an absolute intensity measurement, is used for quantitation of the analyte concentration.[2] The precision of ratios measured by qICP-MS[3–6] usually lies in a range of 0.1–1%. More recent introduction of sector field ICP-MS (SF-ICP-MS) with single or multi-collector detection onto the market has brought a new dimension to this analytical field. In addition to its high mass resolution and high sensitivity, its unique flat topped peaks produced in low resolution mode provide for a more accurate and precise isotope ratio measurement.[7–11] This has been reported to be better than 0.04% precision with a single detector and as low as 0.002% on instruments equipped with a multi-collector detector.

Trace metal speciation analysis has increased dramatically in the last decade due to its important role in assessing the fate of elements in the environment and their impact on biological systems.[12,13] Tributyltin (TBT), for example, has been introduced into the environment by anthropogenic sources. The growing concerns over its toxicity effects and those from dibutyltin (DBT) and monobutyltin (MBT) degradation products entering the environment have led to a dramatic increase in interest in the development of accurate and rapid analytical methods for their determination. Coupling of GC[14–22] or HPLC[23–26] to ICP-MS has provided sensitive and powerful techniques for butyltin determinations. More recently, species specific isotope dilution has been applied to the determination of butyltins[18–20,25–27] and other organometallic species, including organolead[25,26,28] and methylmercury[29–31] for more accurate and precise results, using synthesized species-specific spikes. Among these studies, qICP-MS has been the choice as a detector due to its relatively fast sampling speed for acquiring transient signals and its simplicity in use compared with early SF-ICP-MS instruments. Recent improvements in new magnet technology for SF-ICP-MS (*e.g.*, Element2) have significantly enhanced its scan speed to the point where it is competitive with that of q-ICP-MS.[32]

There are very few applications wherein GC[33–36] or HPLC[32,37,38] has been coupled to SF-ICP-MS for elemental speciation, and none highlighting the advantage of precise ratio measurements offered by SF-ICP-MS when using species specific isotope dilution for calibration. The objective of this study was to investigate the relative performance of GC for separation coupled to SF-ICP-MS and qICP-MS for the determination of TBT and DBT in a sediment using species-specific isotope dilution based on ^{117}Sn enriched TBT and DBT spikes. A reverse spike isotope dilution approach was

performed to quantify enriched ^{117}Sn TBT and DBT concentrations in the mixed spike solution, thereby ensuring the quality of the final results. The method was validated by the determination of TBT and DBT in National Research Council Canada PACS-2 marine sediment CRM. This is the first report of use of GC separation with SF-ICP-MS detection for the accurate and precise ID determination of organotin in environmental samples.

Experimental section

Instrumentation

The SF-ICP-MS instrument used in this work was a ThermoFinnigan Element2 (Bremen, Germany) equipped with a Scott-type double-pass glass spray chamber and a PFA self aspirating nebulizer (Elemental Scientific, Omaha, NE, USA). A plug-in quartz torch with a sapphire injector and a Ag guard electrode were used. Optimization of the Element2 was performed as recommended by the manufacturer.

For comparison purposes, a PerkinElmer SCIEX ELAN 6000 (Concord, Ontario, Canada) qICP-MS equipped with a Gem cross-flow nebuliser and a custom-made quartz sample injector tube (0.9 mm id) were used. A double-pass Ryton® spray chamber was mounted outside the torch box and maintained at room temperature. Optimization of the ELAN 6000 and implementation of dead time correction were performed as recommended by the manufacturer.

A Varian 3400 gas chromatograph (Varian Canada Inc., Georgetown, Ontario, Canada) equipped with an MXT-5 metal column (5% diphenyl, 95% poly(dimethylsiloxane), 20 m × 0.28 mm id with a 0.5 μm film thickness) was used for separation of butyltin species. The GC was coupled to both the SF-ICP-MS and qICP-MS instruments using a home-made interface and transfer line, as described in detail previously.[39] Typical operating conditions for the GC-qICP-MS and GC-SF-ICP-MS systems are summarized in Table 1.

A Microdigest Model 401 (2.45 GHz, maximum power 300 W) microwave digester (Prolabo, Paris, France), equipped with a TX32 programmer, was used for microwave assisted extraction of butyltins from the sediment sample.

A 10 μL liquid sampling syringe (Hamilton Company, Nevada, USA) was used for the injection of samples.

Reagents and solutions

Acetic acid was purified in-house by sub-boiling distillation of reagent grade feedstock in a quartz still prior to use. Environmental grade ammonium hydroxide was purchased from Anachemia Science (Montreal, Quebec, Canada). OmniSolv® methanol (glass-distilled) was purchased from EM Science (Gibbstown, NJ, USA). High purity de-ionized water (DIW) was obtained from a NanoPure mixed bed ion exchange system fed with reverse osmosis domestic feed water (Barnstead/Thermolyne Corp, IA, USA). Sodium tetraethylborate solution, 1% (m/v), was prepared daily by dissolving $NaBEt_4$ (Strem, Bischeim, France) in DIW. A 1 mol l^{-1} sodium acetate buffer was prepared by dissolving an appropriate amount of sodium acetate (Fisher Scientific, Nepean, Ontario, Canada) in water and adjusting the pH to 5 with acetic acid.

Tributyltin chloride (98.3%) and dibutyltin dichloride (97.9%) were purchased from Alfa Products (Danvers, MA, USA). Individual stock solutions of 1000–1500 μg ml^{-1} as tin were prepared in methanol and kept refrigerated until used. The individual TBT and DBT working standard solutions (0.538 and 0.629 μg ml^{-1}) were prepared by diluting the stock solutions with methanol.

^{117}Sn enriched TBT and DBT stock solutions (97% purity), with isotopic compositions and uncertainties provided at nominal concentrations in methanol of 110 μg g^{-1} for both, were supplied by the LGC (Teddington, UK). A mixed spike solution containing approximately 0.12 and 0.18 μg ml^{-1} as tin for TBT and DBT, respectively, was prepared by simple volumetric dilution of the stock in methanol. From previous experience, although the uncertainty contribution from volume measurements is usually larger than the uncertainty arising from mass, the uncertainty contributions from dilutions by volume remain insignificant compared to the total combined uncertainty characterising the overall procedure.[27] Thus, for simplicity in sample preparation, all dilutions were implemented by volume. The concentrations of TBT and DBT in the spike solution were determined by reverse spike isotope

Table 1 GC and ICP-MS operating conditions

	GC	
Injection mode	Splitless	
Injection volume	1 μl	
Injector temperature	250 °C	
Column	MXT-5 (20 m × 0.28 mm × 0.5 μm)	
Carrier gas	He at 32 psi, 1.2 ml min^{-1}	
Oven program	60 °C (1 min) to 200 °C at 20 °C min^{-1}, then to 270 °C at 30 °C min^{-1} (2 min)	
Detector temperature	300 °C	
	ELAN 6000	**Element2**
Rf power	1200 W	1150 W
Plasma Ar gas flow rate	15.0 l min^{-1}	15.0 l min^{-1}
Auxiliary Ar gas flow rate	1.0 l min^{-1}	1.05 l min^{-1}
Ar carrier gas flow rate	0.30 l min^{-1}	0.30 l min^{-1}
Sampler cone (nickel)	1.00 mm	1.1 mm
Skimmer cone (nickel)	0.88 mm	0.8 mm
Lens voltage	7.75 V	Extraction: −2000 V; focus: −870 V; *x* deflection: −2.75 V; *y* deflection: −0.40 V; shape: 105 V
Scanning mode	Peak hopping	
Points per peak	1	
Dwell time	40 ms	
Sweeps per reading	1	
Readings per replicate	5000	
Number of replicates	1	
Dead time	50 ns	17 ns
Resolution		300
Data acquisition		E-scan, 4000 passes, 5% mass window, 60% search window, 60% integration window, 0.0050 s sample time

dilution against the natural abundance TBT and DBT standards.

The marine sediment CRM PACS-2 (NRCC, Ottawa, Canada) was used for validation and the methodology was also applied to the characterization of butyltins in a test sediment.

Sample preparation and analysis procedure

Quantitation of TBT and DBT in sediments and application of reverse spike isotope dilution for quantitation of the ^{117}Sn enriched TBT and DBT spike solution were conducted on the same days. The sediment extraction procedure has been described elsewhere.[23,27] Three sample blanks, four samples of PACS-2 and six replicate samples of test sediment were prepared. Sub-samples of 0.25 g PACS-2 or 0.5 g test sediment along with 0.4560 or 0.1250 ml of ^{117}Sn enriched TBT and DBT (0.12 and 0.18 μg ml^{-1} as tin) spike solution and 10 ml of acetic acid were heated in a Prolabo microwave digester at 60% power for 3 min. The contents were centrifuged at 2000 rpm for 5 min and a 2 ml volume of the supernatant was transferred to a 22 ml glass vial. After 10 ml of 1 mol l^{-1} NaAc buffer solution, 2 ml of ammonium hydroxide, 1 ml of 1% $NaBEt_4$ and 2 ml of isooctane were added, the vial was capped and shaken manually for 5 min. The isooctane layer was then transferred to a 2 ml glass vial for GC-SF-ICP-MS or GC-qICP-MS analysis after phase separation facilitated by centrifuging at 2000 rpm for 5 min.

The concentrations of TBT and DBT in the ^{117}Sn enriched spike were measured by reverse spike isotope dilution against two independently prepared natural TBT and DBT standards. Due to the presence of DBT impurity in the natural abundance TBT standard, and *vice versa*, a reverse spike isotope dilution was performed sequentially for TBT and DBT. For this purpose, a 0.125 ml volume of ^{117}Sn enriched TBT and DBT spike solution was accurately pipetted into each of twelve vials. To the first six vials, 0.1285 ml of 0.538 μg ml^{-1} (or 0.525 μg ml^{-1}) natural abundance TBT solution was added whereas 0.1488 ml of 0.629 μg ml^{-1} (or 0.619 μg ml^{-1}) natural abundance DBT solution was added to the last six vials. After 10 ml of 1 mol l^{-1} NaAc buffer solution, 1 ml of 1% $NaBEt_4$ and 2 ml of isooctane had been added, the mixture was manually shaken for 5 min. Following separation of the phases, the isooctane layer was transferred to a small glass vial and stored in a fridge until the following day for GC-SF-ICP-MS or GC-qICP-MS analysis.

Following injection of the sample onto the GC column, data acquisition on the Elan 6000 or Element2 was manually triggered. Isotopes of ^{120}Sn, ^{118}Sn, and ^{117}Sn were simultaneously monitored. At the end of the chromatographic run, the acquired data were transferred to an off-line computer for further processing using in-house software to yield both peak height and peak area information. In this work, only peak areas were used to generate ^{120}Sn/^{117}Sn ratios, from which the analyte concentration in the sediment was calculated.

Results and discussion

Optimization of GC with SF-ICP-MS

A custom designed[39] easily removable interface and transfer line, shown in Fig. 1, was used to couple the GC to the SF-ICP-MS and qICP-MS instruments. The qICP-MS was first optimised using a standard liquid sample introduction system, the plasma was then extinguished and the spray chamber and nebulizer assembly replaced with the transfer line and its adapter.[39] The final optimization of lens voltage, rf power and Ar carrier gas flow for dry plasma conditions was accomplished by injection of 1 μl of a 50 ng ml^{-1} ethylated butyltin standard in isooctane.

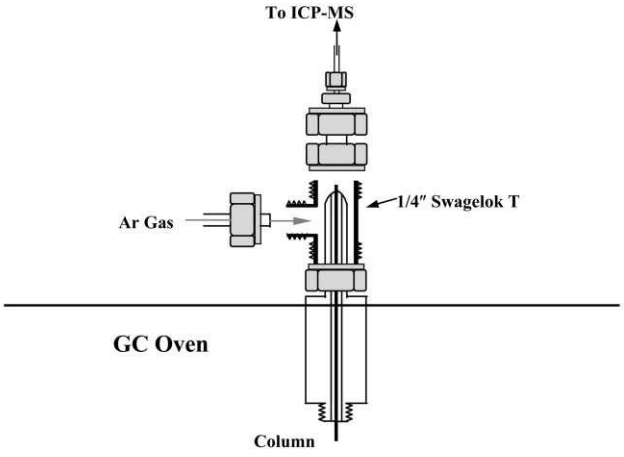

Fig. 1 Schematic diagram of the GC-SF-ICP-MS interface.

Optimization of the SF-ICP-MS system was undertaken as recommended by the manufacturer using liquid sample introduction of a 1 ppb multi-element standard to achieve stable and high sensitivity for Li, In and U. Low resolution (300) was used to achieve best sensitivity and flat topped peaks. Dead time correction was performed as recommended by the manufacturer, based on use of three different concentrations of U. A dead time of 17 ns was obtained. Mass calibration was only performed once a week as a result of the stable mass calibration achievable with the Element2. The plasma was then extinguished and the spray chamber and nebulizer assembly replaced with the transfer line and its ball joint adapter. The final optimization of lens voltages, torch position and RF power for dry plasma conditions was performed by monitoring the ^{129}Xe signal arising from the blending of a small amount of Xe into the Ar carrier gas through a T-connection. No significant difference in parameters for lens voltages, torch position and rf power was evident between wet and dry plasma conditions.

The optimum Ar carrier gas flow rate is dependent on that of the He effluent from the GC column as the Ar was introduced through the side arm of the interface. Therefore, an approach based on monitoring ^{129}Xe under dry plasma conditions was not successful for the optimisation of Ar carrier gas flow. The effect of He pressure (a surrogate for flow rate) on response was investigated by injection of 1 μl of a 25 ng ml^{-1} standard of ethylated butyltin in isooctane. A significant effect of He pressure on butyltin retention time was observed, the latter decreasing as He pressure increased and separation slightly deteriorated. A peak for TBT was not obtained when the He pressure was reduced below 20 psi. A He pressure of 32 psi was selected for producing the shortest retention time for butyltin while maintaining good separation. An Ar carrier gas flow rate in the range of 0.2–1.2 l min^{-1} was investigated using a He pressure of 32 psi. Highest sensitivities were found using an Ar carrier gas flow rate in the range of 0.280–0.32 l min^{-1}; sensitivities decreased significantly at either lower or higher Ar carrier gas flows. Thus, an optimum Ar carrier gas flow rate of 0.30 l min^{-1} was selected for the dry plasma conditions, resulting in a He flow rate of 1.2 ml min^{-1} under the chosen conditions. The optimum Ar carrier gas flow rate obtained is significantly different from the optimum flow rate of 1.20 l min^{-1} used with wet plasma conditions. A further study was conducted to determine whether a make-up gas, introduced through a T connection at the end of transfer line to the torch (to avoid any pressure build up at the end of GC column at the interface), would improve sensitivities. No significant improvement was observed as make up gas flow rate

was increased from 0.1 to 1.1 l min^{-1}, producing a total sample Ar flow rate of 0.4–1.4 l min^{-1}.

As a result of the above studies, optimization of the GC-SF-ICP-MS system was simplified for ease of operation in the final study. The Element2 liquid sample introduction system was brought on line once a week to optimize the instrument and conduct mass calibration. It was then removed to permit GC sample introduction. Ar carrier gas flow rate was then optimized by injection of a 25 ng ml^{-1} butyltin standard in isooctane using a He pressure setting of 32 psi. No change in day to day optimum Ar carrier gas flow rate was observed when using the same He pressure setting and similar transfer line length.

It is worth noting that the length of the transfer line had little effect on either the butyltin peak shape or sensitivity, due to the short analyte residence time. Therefore, for flexibility and ease of handling of the GC-SF-ICP-MS, a 100 cm long PTFE line was used for the final work. It was necessary to change this PTFE tubing daily to minimize significant broadening of TBT peaks. Evidently, a surface residue accumulates over the course of the day in this unheated line. No significant influence of the distance between the injector tip and the end of the transfer line on the resulting sensitivity was observed in the range 0-12 mm. However, plasma instability was noted when the distance was greater than 15 mm when isooctane extract was injected. A 5 mm distance was selected for this study.

As is evident in Fig. 2, good resolution and peak profiles for all three ethylated butyltin species were obtained under optimized conditions using this home-made interface and transfer line with GC-SF-ICP-MS. The peak widths ranged from 2 to 5 s at 10% height, comparable to those obtained using conventional GC detectors with the given temperature program. Chromatograms obtained using qICP-MS for detection suffered from a 10-fold poorer sensitivity than those for SF-ICP-MS. With the data acquisition parameters used, all peaks were reliably recorded using SF-ICP-MS without distortion, despite their narrow half widths. An example of this is presented in Fig. 3, wherein a segment of the recorded chromatograms illustrating the narrow DBT ^{120}Sn peak is presented for both detection systems. More that 40 data points characterize the peak in the SF-ICP-MS chromatogram, which has a full width at half maximum (FWHM) of only 2.0 s. It is clear that the temporal characteristics of this peak are identical to those recorded

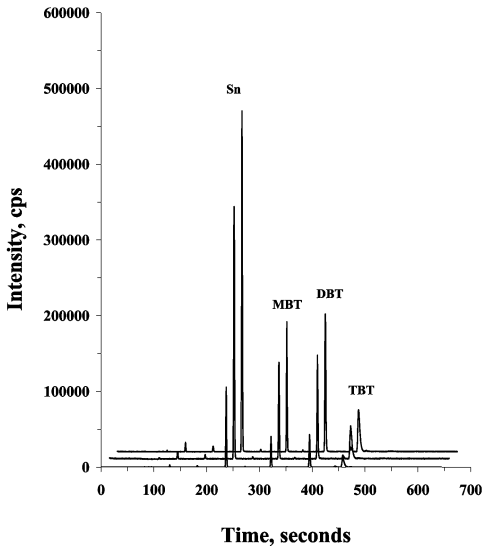

Fig. 2 Chromatogram of unspiked test sediment extract obtained by GC-SF-ICP-MS (with ^{117}Sn, ^{118}Sn and ^{120}Sn traces, ^{118}Sn and ^{120}Sn traces shifted for clarity).

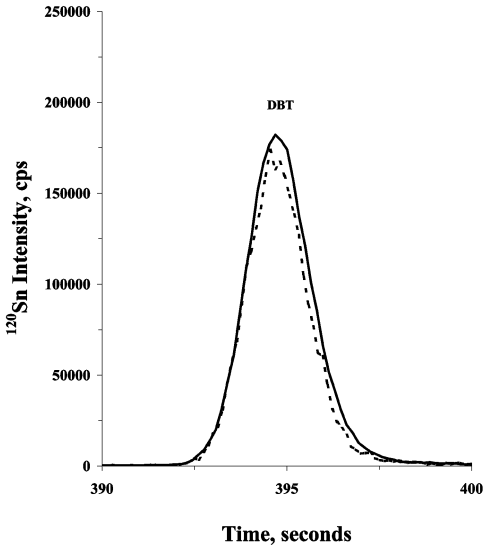

Fig. 3 Segment of chromatograms from a test sediment extract showing the DBT (^{120}Sn) peak obtained by GC-SF-ICP-MS (solid line) and GC-qICP-MS (broken line). For comparative purposes, the qICP-MS signal intensity has been enhanced 9.5-fold and has been shifted 4.2 s to achieve a retention time match so as to permit temporal overlap of the peaks.

using qICP-MS detection. The rapid mass scanning capability of SF-ICP-MS (Element2) thus offers no impediment to the accurate recording of transient signals.

Ratio measurements for TBT and DBT using GC-SF-ICP-MS and GC-qICP-MS

Dead time correction is important for achieving accurate ratio measurements. Seventeen and 50 ns dead time corrections were evaluated for the SF-ICP-MS (Element2) and qICP-MS (ELAN6000), respectively, derived from procedures recommended by the manufacturers when using liquid sample introduction. Ratios of $^{120}Sn/^{117}Sn$ for the butyltin standards in the concentration range of 10–200 ng ml^{-1} in isooctane were measured with both GC-SF-ICP-MS and GC-qICP-MS to investigate if dead time corrections were adequate for butyltin determinations. Mass bias correction factors were determined based on the assumed natural abundance ratio of $^{120}Sn/^{117}Sn$ (4.246) divided by the mean value of $^{120}Sn/^{117}Sn$ obtained from inorganic Sn peaks calculated for all injected standards. A mass bias correction factor of 0.9942 $\pm$ 0.0047 (one standard deviation, $n = 16$) for $^{120}Sn/^{117}Sn$ was obtained using the Element2, significantly smaller than 0.970 $\pm$ 0.011 (one standard deviation, $n = 16$) obtained with the ELAN6000. Mass bias corrected $^{120}Sn/^{117}Sn$ ratios for TBT and DBT in standard solutions in the concentration range 10–200 ng ml^{-1} are reported in Table 2. No significant difference was found for calculated ratios at different concentrations, suggesting that the dead time corrections used are adequate for both instruments.

As noted earlier, the Element2 produces flat topped peaks at low resolution, thereby permitting more accurate and precise ratio measurements. As expected, a precision of 0.25–0.75% RSD in the calculated $^{120}Sn/^{117}Sn$ ratios obtained using GC-SF-ICP-MS is significantly better than the 0.70 to 1.6% RSD obtained using GC-qICP-MS. This is a direct consequence of the enhanced sensitivity improving the counting statistics.

Determination of TBT and DBT in sediment using ID-GC-SF-ICP-MS and GC-qICP-MS

As noted earlier, ID-MS is capable of compensating for any loss of analyte during subsequent sample preparation, suppression of ion intensities by concomitant elements present

Table 2 Ratio results with GC-SF-ICP-MS and GC-qICP-MS

	Measured ratios, $^{120}Sn/^{117}Sn$ ($n = 4$)			
	GC-SF-ICP-MS		GC-qICP-MS	
Sample name	DBT	TBT	DBT	TBT
10 ppb	4.231 ± 0.025	4.244 ± 0.032	4.241 ± 0.060	4.244 ± 0.051
50 ppb	4.237 ± 0.010	4.254 ± 0.024	4.241 ± 0.067	4.253 ± 0.039
100 ppb	4.250 ± 0.020	4.247 ± 0.016	4.242 ± 0.054	4.248 ± 0.035
200 PPb	4.242 ± 0.020	4.245 ± 0.016	4.246 ± 0.040	4.246 ± 0.031
Test sediment	4.248 ± 0.038	4.245 ± 0.024	4.250 ± 0.060	4.247 ± 0.058

in the sample matrix and for instrument drift, providing isotopic equilibration is achieved between the added spike and the endogenous analyte in the sample. In addition, an interference-free pair of isotopes must be available for ratio measurements, care must be taken to avoid any contamination during the process, and an optimum measurement procedure must be used to achieve accurate ratio measurements.

In practice, validation of the achievement of equilibration of the enriched spike and the endogenous analyte in the sample is not easy. Previous studies[17,23] revealed that, despite a difference in the spike recoveries (100% for both TBT and DBT for sample weights of 0.5 g, and 83 and 84%, respectively, using 2.0 g), there was no significant difference in TBT and DBT concentrations measured in PACS-2 CRM control material using a standard additions calibration approach. These data suggest that the added spike fully mimics the analyte in the sample during the microwave extraction process.

Although both isotope pairs of $^{120}Sn/^{117}Sn$ and $^{118}Sn/^{117}Sn$ can be used for the quantitation of butyltins, $^{120}Sn/^{117}Sn$ was selected because of enhanced sensitivity. As shown in Table 2, both mass bias corrected $^{120}Sn/^{117}Sn$ ratios measured in the unspiked test sediment using GC-SF-ICP-MS and GC-qICP-MS are not significantly different from the expected value of 4.246, confirming that no significant spectroscopic interference arises on either isotope from sample matrix components, permitting accurate results to be obtained using the chosen isotope pair.

Mass bias correction can be achieved based on data derived either by injection of natural butyltin standards or by using the inorganic Sn peak in the chromatogram of each sample. The latter approach not only saves analysis time, but also provides better correction since instrument drift is accounted for with each sample. A $^{120}Sn/^{117}Sn$ ratio of 4.266 ± 0.028 (one standard deviation, $n = 22$) was obtained based on inorganic Sn peaks in chromatograms of all injected samples, in good agreement with ratios of 4.267 ± 0.025 and 4.271 ± 0.017 (one standard deviation, $n = 6$) obtained for TBT or DBT in the natural butyltin standards. This suggests that the inorganic Sn peak in the chromatogram of each sample can be used to calculate the mass bias correction factor. The following equation was used for the quantitation of TBT and DBT in the test sediment:

$$C_x = C_z \cdot \frac{v_y}{w \cdot m_x} \cdot \frac{v_z}{v'_y} \cdot \frac{A_y - B_y \cdot R_n}{B_{xz} \cdot R_n - A_{xz}} \cdot \frac{B_{xz} \cdot R' - A_{xz}}{A_y - B_y \cdot R'_n} - C_b \qquad (1)$$

where C_x is the blank corrected analyte concentration as Sn (μg g^{-1}) based on dry mass; C_z is the concentration of natural abundance butyltin standard (μg ml^{-1}); v_y is the volume (ml) of spike used to prepare the blend solution of sample and spike; m_x is the mass (g) of sample used; w is the dry mass correction factor; v_z is the volume (ml) of natural abundance butyltin standard used; v'_y is the volume (ml) of spike used to prepare the blend solution of spike and natural abundance butyltin standard solution; A_y is the abundance of the reference isotope (^{120}Sn) in the spike; B_y is the abundance of the spike isotope (^{117}Sn) in the spike; A_{xz} is the abundance of the reference isotope in the sample or in the standard; B_{xz} is the abundance of the spike isotope in the sample or in the standard; R_n is the measured reference/spike isotope ratio (mass bias corrected) in the blend solution of sample and spike; R'_n is the measured reference/spike isotope ratio (mass bias corrected) in the blend solution of spike and natural abundance butyltin standard; and C_b is the blank concentration (μg g^{-1}). The mass bias correction factor of 0.9952 ± 0.0065 (mean and one standard deviation, $n = 22$) for $^{120}Sn/^{117}Sn$ based on inorganic Sn response in all injected samples was obtained, indicating no significant mass bias drift during a run sequence. Concentrations of 0.1244 ± 0.0020 and 0.1813 ± 0.0029 μg g^{-1} (one standard deviation, $n = 6$) as Sn for TBT and DBT, respectively, were obtained in the test sediment using the average mass bias correction factor of 0.9952, in good agreement with values of 0.1243 ± 0.0022 and 0.1812 ± 0.0032 μg g^{-1} using individual mass bias correction factors for each sample.

A subsequent comparative analysis of this sediment was performed using GC-qICP-MS. Concentrations of 0.1248 ± 0.0021 and 0.1794 ± 0.0059 μg g^{-1} (one standard deviation, $n = 6$) as Sn for TBT and DBT, respectively, were obtained using an average mass bias correction factor of 0.9696 ± 0.0089 (mean and one standard deviation, $n = 22$) obtained from the inorganic Sn peaks. As expected, slightly better precisions of 1.59–1.62% RSD in measured butyltin concentrations were obtained by GC-SF-ICP-MS compared with 1.64–3.31% RSD obtained with the GC-qICP-MS approach.

Method detection limits (LODs based on three times the standard deviation of the blanks) for ID-GC-SF-ICP-MS and GC-qICP-MS techniques were calculated using three measurements on ^{117}Sn TBT and DBT spiked sample blanks. It should be noted that detection limits could, in principle, be enhanced 5-fold if the entire 10 ml extract was taken for derivatization. Values of 0.4 and 0.3 ng g^{-1} for TBT and DBT, respectively, were obtained using GC-SF-ICP-MS, based on a 0.5 g sample. These are superior to LODs of 0.9 and 1.0 ng g^{-1} obtained using GC-qICP-MS. Although sensitivities for TBT and DBT using GC-SF-ICP-MS were 10-fold better than those arising with GC-qICP-MS, only a 2-fold improvement in method LODs arose, most likely due to a constant and high, but unidentified, background observed at m/z ^{120}Sn using SF-ICP-MS.

Validation of isotope dilution GC-SF-ICP-MS and GC-qICP-MS methods for the determination of TBT and DBT

Sediment CRM PACS-2 was used to validate the proposed method. Concentrations of 0.883 ± 0.013 and 1.126 ± 0.013 μg g^{-1} (mean and one standard deviation, $n = 4$) as tin were obtained for TBT and DBT, respectively, by GC-SF-ICP-MS, in agreement with certified values of 0.98 ± 0.13 and 1.09 ± 0.15 μg g^{-1} (95% confidence interval) for these species. Concentrations of 0.883 ± 0.019 and 1.116 ± 0.014 μg g^{-1} (mean and one standard deviation, $n = 4$) as tin were obtained for TBT and DBT, respectively, by GC-qICP-MS.

More than a 2-fold improvement in precision of measured

$^{120}Sn/^{117}Sn$ ratios for both TBT and DBT in the butyltin standards was obtained using GC-SF-ICP-MS, as compared with GC-qICP-MS. A similar improvement in the precision of measurement of resulting TBT and DBT concentrations in both the test sediment and PACS-2 CRM was not realized. This may be due to limitations in the homogeneity of the samples or variability contributed by the sample preparation procedures.

Conclusion

A sensitive method is described for the accurate and precise determination of TBT and DBT in sediments by species specific isotope dilution using both qICP-MS and GC-SF-ICP-MS. A 2-fold enhancement in the precision of TBT and DBT Sn isotope ratios measured in standard solutions by GC-SF-ICP-MS, as opposed to GC-qICP-MS, was obtained. This advantage is not realized when real samples are processed because the variability introduced with the additional steps of sample preparation and inhomogeneity become the major contributors to the overall imprecision of the results. A 3-fold improvement in their LODs was observed as a consequence of the enhanced sensitivity realized with the sector field instrument. The rapid mass scanning capability of the SF-ICP-MS, contrary to currently perceived notions, offered no impediment to rapid peak hopping for the accurate recording of transient signals having FWHM of only a few seconds.

Acknowledgements

The authors thank LGC Ltd. (Teddington, UK) for providing the ^{117}Sn enriched TBT and DBT spike solutions.

References

1 K. E. Jarvis, A. L. Date and R. S. Houk, *Handbook of Inductively Coupled Plasma Mass Spectrometry*, Blackie, Glasgow, 1992.
2 P. De Bièvre, *Isotope Dilution Mass Spectrometry in Trace Element Analysis in Biological Specimens*, ed. R. F. M. Herber and M. Stoeppler, Elsevier, 1994.
3 N. J. Furuta, *J. Anal. At. Spectrom.*, 1991, **6**, 199–203.
4 M. E. Ketterer, *J. Anal. At. Spectrom.*, 1992, **7**, 1125–1129.
5 S. R. Koirtyohann, *Spectrochim. Acta, Part B*, 1994, **49**, 1305–1311.
6 R. Roehl, J. Gomez and L. R. Woodhouse, *J. Anal. At. Spectrom.*, 1995, **10**, 15–23.
7 C. Latkoczy, T. Prohaska, G. Stingeder and M. Teschler-Nicola, *J. Anal. At. Spectrom.*, 1998, **13**, 561–566.
8 F. Vanhaecke, L. Moens and R. Dams, *Anal. Chem.*, 1996, **68**, 567–569.
9 C. R. Quétel, T. Prohaska, M. Hamester, W. Kerl and P. D. P. Taylor, *J. Anal. At. Spectrom.*, 2000, **15**, 353–358.
10 M. Rehkämper and K. Mezger, *J. Anal. At. Spectrom.*, 2000, **15**, 1451–1460.
11 A. Galy, C. Pomiès, J. A. Day, O. S. Polrovsky and J. Schott, *J. Anal. At. Spectrom.*, 2003, **18**, 115–119.
12 P. J. Craig, *Organometallic Compounds in the Environment: Principles and Reactions*, Harlow, Essex, England, 1986.
13 M. A. Champ and P. F. Seligman, *Organotin Environmental Fate and Effects*, Chapman and Hall, 1996.
14 L. Moens, T. De Smaele, R. Dams, P. Van den Broeck and P. Sandra, *Anal. Chem.*, 1997, **69**, 1604–1611.
15 S. Aguerre, G. Lespes, V. Desauziers and M. Potin Gautier, *J. Anal. At. Spectrom.*, 2001, **16**, 263–269.
16 T. De Smaele, L. Moens, R. Dams and P. Sandra, *Fresenius' Anal. Chem*, 1996, **355**, 778–782.
17 M. M. Bayon, M. G. Camblor, J. I. García Alonso and A. Sanz-Medel, *J. Anal. At. Spectrom.*, 1999, **14**, 1317–1322.
18 J. Ruiz Encinar, J. I. García Alonso and A. Sanz-Medel, *J. Anal. At. Spectrom.*, 2000, **15**, 1233–1239.
19 J. Ruiz Encinar, P. R. Gonzalez, J. I. García Alonso and A. Sanz-Medel, *Anal. Chem.*, 2002, **74**, 270–281.
20 J. Ruiz Encinar, M. I. Monterde Villar, V. Gotor Santamaría, J. I. García Alonso and A. Sanz-Medel, *Anal. Chem.*, 2001, **73**, 3174–3180.
21 R. B. Rajendran, H. Tao, T. Nakazato and A. Miyazaki, *Analyst*, 2000, **125**, 1757–1763.
22 H. Tao, R. B. Rajendran, C. R. Quetel, T. Nakazeto, M. Tominaga and A. Miyazaki, *Anal. Chem.*, 1999, **71**, 4208–4215.
23 L. Yang and J. W. H. Lam, *J. Anal. At. Spectrom.*, 2001, **16**, 724–731.
24 S. Chiron, S. Roy, R. Cottier and R. Jeannot, *J. Chromatogr. A*, 2000, **879**, 137–145.
25 S. J. Hill, A. Brown, C. Rivas, S. Sparkes and L. Ebdon, in *Quality Assurance for Environmental Analysis*, ed. Ph. Quevauviller, E. A. Maier and B. Griepink, Elsevier, 1995, ch. 16.
26 S. J. Hill, L. J. Pitts and A. S. Fisher, *Trends Anal. Chem.*, 2000, **19**, 120–126.
27 L. Yang, Z. Mester and R. Sturgeon, *Anal. Chem.*, 2002, **74**, 2968–2976.
28 L. Ebdon, S. J. Hill and C. Rivas, *Spectrochim. Acta, Part B*, 1998, **53**, 289–297.
29 N. Demuth and K. G. Heumann, *Anal. Chem.*, 2001, **73**, 4020–4027.
30 C. M. Barshick, S. M. Barshick, E. B. Walsh, M. A. Vance and P. F. Britt, *Anal. Chem.*, 1999, **71**, 483–488.
31 L. Yang, Z. Mester and R. E. Sturgeon, *J. Anal. At. Spectrom.*, 2003 in the press.
32 ELEMENT2 Thermo Finnigan Application Flash Report No. E15, ThermoFinnigan Nov., 2002.
33 J. Rodríguez-Fernández, M. Montes-Bayón, R. Pereiro and A. Sanz-Medel, *J. Anal. At. Spectrom.*, 2001, **16**, 1051–1056.
34 M. Edler, D. Metze, N. Jakubowski and M. Linscheid, *J. Anal. At. Spectrom.*, 2002, **17**, 1209–1212.
35 E. M. Krupp, C. Pécheyran, H. Pinaly, M. Motelica-Heino, D. Koller, S. M. M. Young, I. B. Brenner and O. F. X. Donard, *Spectrochim. Acta, Part B*, 2001, **56**, 1233–1240.
36 E. M. Krupp, C. Pécheyran, S. Meffan-Main and O. F. X. Donard, *Fresenius' Anal. Chem.*, 2001, **370**, 573–580.
37 G. Koellensperger, J. Numi, S. Hann, G. Stingeder, W. J. Fitz and W. W. Wenzel, *J. Anal. At. Spectrom.*, 2002, **17**, 1042–1047.
38 M. Wind, M. Edler, N. Jakubowski, M. Linscheid, H. Wesch and W. D. Lehmann, *Anal. Chem.*, 2001, **73**, 29–35.
39 L. Yang, Z. Mester and R. E. Sturgeon, *J. Anal. At. Spectrom.*, 2002, **17**, 944–949.